DOI: 10.1021/ma1017764

Macromolecules
ARTICLE

In-Situ Generation of a Dispersion of POSS Crystalline Platelets in an Epoxy Matrix Induced by Polymerization

C. Di Luca, E. R. Soulé, I. A. Zucchi,* C. E. Hoppe, L. A. Fasce, and R. J. J. Williams*

Institute of Materials Science and Technology (INTEMA), University of Mar del Plata and National Research Council (CONICET), J. B. Justo 4302, 7600 Mar del Plata, Argentina

Received August 3, 2010; Revised Manuscript Received September 6, 2010

ABSTRACT: The dispersion of intercalated/exfoliated clays in polymers imparts some desired properties to the neat matrix, such as a decrease in permeability due to geometrical effects and an increase in the fire resistance due to the inorganic character of the clay. However, processing is difficult mainly due to the high viscosities of the starting dispersions. In this article we explored the possibility of producing a dispersion of crystalline platelets in situ during polymerization, starting from homogeneous solutions. For this purpose, we replaced the clays with polyhedral oligomeric silsesquioxanes (POSS) because they can be dissolved in adequate polymer precursors and can be phase-separated in the course of polymerization. The aim was to find conditions where a crystal−liquid (C−L) phase separation could take place instead of a conventional L−L phase separation. The in-situ generation of POSS crystalline platelets can impart similar characteristics to those observed in clay-modified polymers (except for the nanoscopic size of thickness), with the advantage of a much easier processing. The selected formulation was based on glycidyloxypropyl-heptaisobutyl POSS dissolved in a stoichiometric mixture of diglycidyl ether of bisphenol A (DGEBA) and 4,4′-methylenebis(2,6-diethylaniline) (MDEA). In a specific range of POSS concentrations and polymerization temperatures, a C−L phase separation was observed generating POSS crystalline platelets with sizes in the range of the micrometers. Following this primary phase separation, a dispersion of POSS-rich droplets was produced when the residual liquid phase entered the L−L immiscibility region. The final material exhibited a dual dispersion of POSS platelets and spherical POSS-rich domains uniformly dispersed in the matrix. A thermodynamic model enabled to provide an explanation of the experimental observations.

Introduction

The dispersion of intercalated/exfoliated clays in polymers imparts some desired characteristics to the neat matrix such as a decrease in permeability due to geometrical effects and an increase in fire resistance. However, processing is difficult mainly due to the high viscosities of the starting dispersions and the need to keep a homogeneous dispersion throughout the process. In this article we explored the possibility of changing the top-down approach (intercalation plus exfoliation) by a bottom-up approach consisting of producing the dispersion of crystalline platelets in situ during polymerization, starting from a homogeneous solution. For this purpose we replaced the clays with a polyhedral oligomeric silsesquioxane (POSS) based on the idea that POSS can be dissolved in adequate polymer precursors and can be phase-separated in the course of polymerization by a conventional liquid−liquid (L−L) phase separation.[1−5] The aim of this study was to manage the polymerization conditions so that the material could be conveyed to a crystal−liquid (C−L) immiscibility region, producing the phase separation of POSS crystals in the course of polymerization. This kind of phase separation has been reported for epoxies modified by poly(butylene terephthalate) (PBT),[6,7] poly(oxymethylene) (POM),[8−10] syndiotactic polystyrene,[11] and gold nanoparticles.[12] However, to the best of our knowledge, it has not been reported for POSS-modified thermosetting polymers. The generation of POSS crystalline platelets can impart similar characteristics to the material as those obtained with the use of conventional clays (except for the nanoscopic size of thickness), with the advantage of a much easier processing.

*To whom correspondence should be addressed. E-mail: ileanazu@yahoo.com.ar (I.A.Z.); williams@fi.mdp.edu.ar (R.J.J.W.).

A particular POSS−epoxy system where a typical L−L phase separation induced by polymerization had been previously reported[5] was selected to analyze conditions where a C−L phase separation could be produced. When the formulation was polymerized under appropriate conditions, micrometer-size POSS crystalline platelets were generated. This process was followed by an L−L phase separation producing POSS-rich droplets. The cured epoxy exhibited a dual dispersion of POSS crystalline platelets and spherical domains rich in POSS. A thermodynamic model provided an explanation of the two-step phase separation process.

Experimental Section

Materials. The diepoxy monomer was based on diglycidyl ether of bisphenol A (DGEBA, DER 332, Dow), with a mass per mole of epoxy groups equal to 174.3 g/mol ($n = 0.03$ in the chemical structure shown in Figure 1) and a mass density of 1.17 g/cm^3. The hardener was 4,4′-methylenebis(2,6-diethylaniline) (MDEA, Aldrich), a crystalline solid with a molar mass of 310.5 g/mol, a mass density of 1.02 g/cm^3, and a melting temperature of 96.5 °C. Glycidyloxypropyl-heptaisobutyl POSS (iBu-Gly-POSS, EPO 418 Hybrid Plastics) was a crystalline powder with a molar mass of 931.6 g/mol and a mass density of 1.14 g/cm^3. Two well-defined melting peaks at 112 and 132 °C are present in DSC (differential scanning calorimetry) thermograms of the commercial product.[1] After melting and recrystallization in mass, these peaks are shifted to 123 and 149 °C, with a total melting heat of 15.9 J/g.[1] Chemical structures of MDEA and POSS are also shown in Figure 1.

Polymerization Conditions. The desired amount of POSS was dissolved in DGEBA at an appropriate temperature to obtain a homogeneous solution. Then, the stoichiometric amount of

 Published on Web 10/06/2010

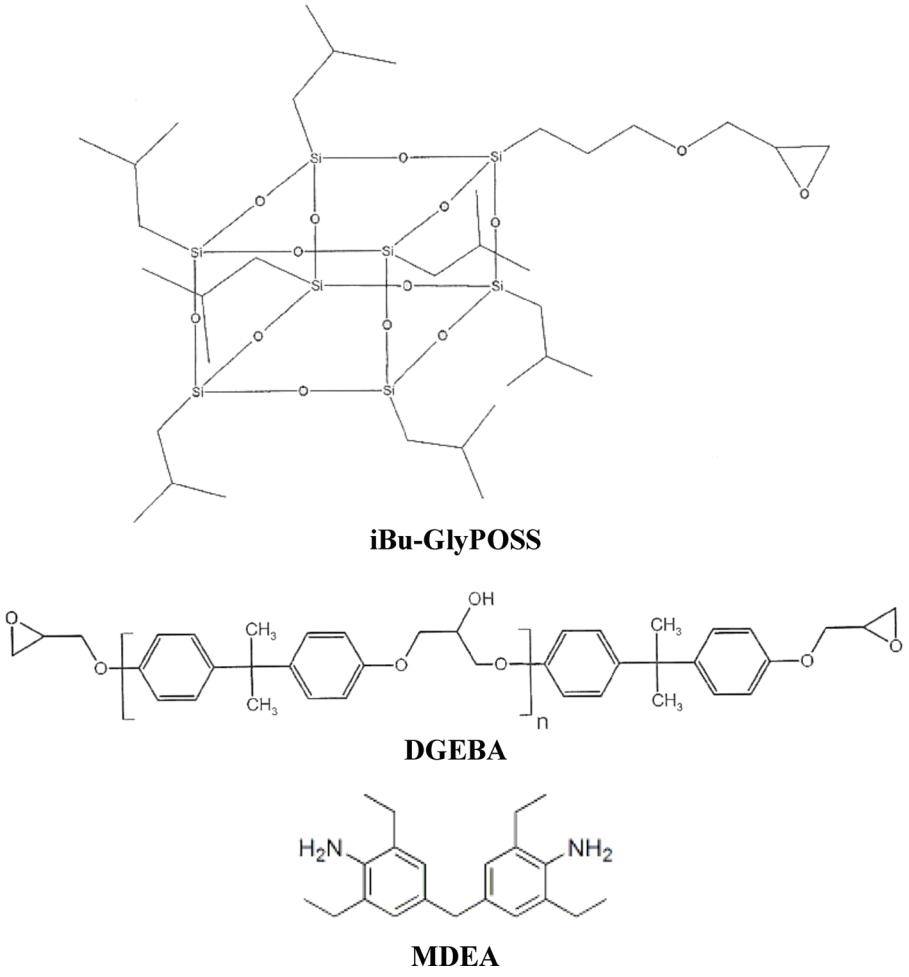

Figure 1. Chemical structures of DGEBA, MDEA, and iBu-GlyPOSS.

MDEA calculated with respect to the epoxy functionalities contributed by DGEBA was added under continuous stirring (as the epoxy group of POSS reacts at a very much slower rate with MDEA than the epoxy groups of DGEBA,[5] POSS acts as a nonreactive modifier of the DGEBA−MDEA system). The polymerization was performed at either 115 or 135 °C for several hours to surpass the gel conversion (about 0.60). When complete conversion was desired, a postcure at 190 °C for 4 h was carried out.

Techniques. Transmission optical microscopy (TOM) was employed to determine cloud-point temperatures of POSS−DGEBA and POSS−DGEBA/MDEA blends before reaction, phase separation times during polymerization, and the evolution of generated morphologies. A Leica DMLB microscope provided with a video camera (Leica DC 100) and a hot stage (Linkam THMS 600) was used for these purposes. Samples were placed between two glasses using a 0.5 mm stainless steel spacer and a 50 μm adhesive tape spacer.

Morphologies of final materials were observed by scanning electron microscopy (SEM, Jeol 6460 LV, fracture surfaces were coated by a fine gold layer).

Fourier-transformed near-infrared spectroscopy (FT-NIR) was used to determine conversion vs time curves at 115 and 135 °C for the neat epoxy−amine formulation. A Nicolet 6700 FTIR device, equipped with a heated transmission cell (HT-32, Spectra Tech) with glass windows (32 mm diameter, 1 mm rubber spacer) and a programmable temperature controller (Omega, Spectra Tech, DTZG1 8C), was employed. The conversion of epoxy groups was followed by measuring the height of the absorption band at 4530 cm^{-1} with respect to the height of a reference band at 4620 cm^{-1}.

Differential scanning calorimetry (DSC) was performed with Pyris 1 Perkin- Elmer and DSC50 Shimadzu devices. Thermograms were obtained at a scanning rate of 20 °C/min.

Results and Discussion

Cloud-Point Curve of POSS−DGEBA Blends. The miscibility curve was determined using TOM at a cooling rate of 5 °C/min. Results are shown in Figure 2. It is observed that POSS was quite immiscible with DGEBA, and it was necessary to heat to relatively high temperatures to get an initial homogeneous solution of POSS in DGEBA.

Phase Separation in POSS−DGEBA/MDEA Blends before Reaction. TOM at a cooling rate of 5 °C/min was employed to determine the miscibility range for the initial formulation. Crystallization of POSS from the homogeneous solution was clearly identified by the appearance of large crystals, as observed in Figure 3 (0.5 mm spacer). A subsequent liquid−liquid phase separation was also observed generating spherical droplets in the sample. For a range of POSS concentrations, C−L and L−L phase separation processes were observed in series when cooling the initial homogeneous solution. Phase-separated samples were reheated in the DSC to obtain the melting temperature of POSS crystals, defined at the end of the melting peak.

Figure 4 shows a temperature vs composition phase diagram of the POSS−DGEBA/MDEA blend before reaction, including the L−L immiscibility region and melting and crystallization temperatures of POSS. The crystallization curve depends on the cooling rate, but it is shown to indicate

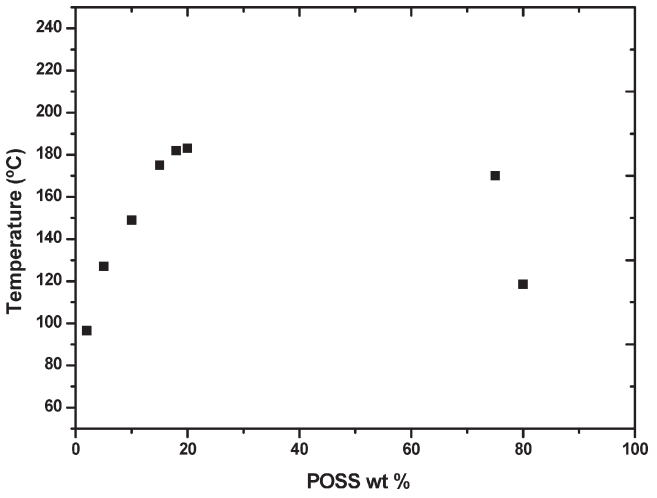

Figure 2. Miscibility of POSS−DGEBA binary blends.

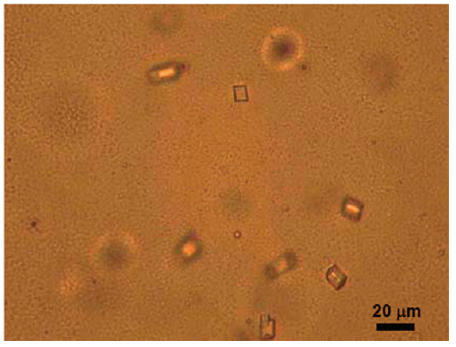

Figure 3. Generation of large POSS crystals observed when cooling a POSS−DGEBA/MDEA blend containing 7.5 wt % POSS before reaction.

the necessary overcooling to generate POSS crystals with a size that could be observed by TOM. The addition of MDEA to the binary POSS−DGEBA blend produced an increase in miscibility, observed by comparing Figures 2 and 4.

Two polymerization temperatures, 115 and 135 °C, were selected on the basis of the phase diagram shown in Figure 4. Using POSS concentrations in the range of 0−15 wt % enabled to obtain initial homogeneous solutions at 135 °C. The range of POSS concentrations giving homogeneous solutions was reduced at 115 °C. Strictly stable homogeneous solutions located above the melting curve at 115 °C were those with POSS concentrations below 7.5 wt %. However, solutions containing up to 10 wt % POSS were homogeneous at 115 °C during the time necessary to prepare the blends and start the polymerization reaction. Therefore, the 0−10 wt % range of POSS concentrations was employed for samples polymerized at 115 °C.

Both the C−L and L−L immiscibility regions are shifted to higher temperatures with an increase in the conversion of the polymerization reactions (see the Thermodynamic section). At a particular conversion, one of these curves will reach the point identifying the sample composition and the polymerization temperature. As the system enters the metastable region, a phase separation process will start to take place. From the shape of the C−L and L−L curves, we can reasonably expect that an L−L phase separation will take place at 135 °C while a C−L phase separation will occur at 115 °C. This is the reason for selecting these two temperatures to analyze the morphologies generated in the course of polymerization.

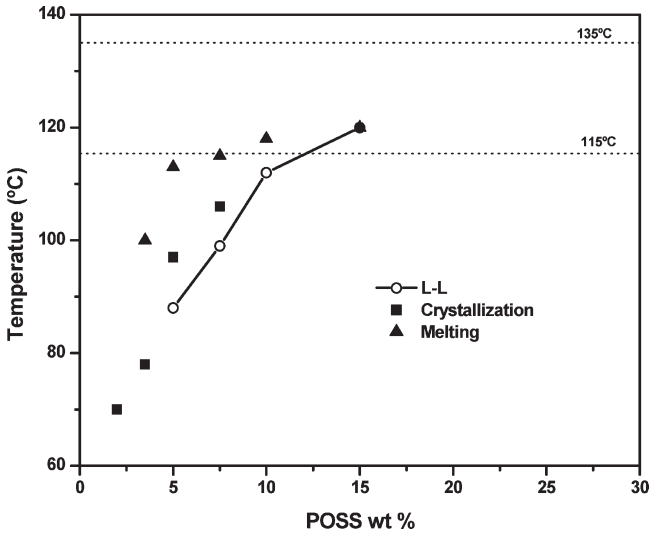

Figure 4. Temperature vs composition phase diagram of the POSS−DGEBA/MDEA blend before reaction, including the L−L immiscibility region and melting and crystallization temperatures of POSS.

Polymerization-Induced Phase Separation in POSS−DGEBA/MDEA Blends. We have previously reported that a typical L−L phase separation takes place at 135 °C for a blend containing 8.4 wt % POSS.[5] This finding was confirmed by curing blends containing 5, 10, and 15 wt % POSS at 135 °C up to conversions close to 0.60 (4 h as results from the conversion vs time curve determined by FT-NIR, provided as Supporting Information) and postcuring at 190 °C to complete the reaction. SEM micrographs showing the resulting morphologies are presented in Figure 5a−c.

The diameter of POSS-rich dispersed droplets increased from 1.8 μm (5 wt % POSS) to 4.5 μm (10 wt % POSS) and to 7.1 μm (15 wt % POSS). These are typical results of a polymerization-induced L−L phase separation through a nucleation−growth−coarsening mechanism.[13] The cooling of these samples to room temperature produced the partial crystallization of POSS inside the droplets.

Figure 6 shows DSC thermograms of the cured DGEBA/MDEA matrix and the cured blend containing 15 wt % POSS. The melting peak of POSS crystals is evidenced by the endothermic peak with a minimum at about 135 °C. Taking into account the heat of fusion of pure POSS (15.9 J/g),[1] the fraction of crystalline POSS was 29%. The glass transition temperature of the POSS-modified blend was about 10 °C lower than the one of the pure matrix due to the POSS fraction remaining dissolved in the matrix.

The development of morphologies was completely different when the polymerization was carried out at 115 °C. Figure 7 shows a sequence of the evolution of morphologies observed by TOM for a blend containing 5 wt % POSS (50 μm spacer). At about 170 min a crystal−liquid (C−L) phase separation was first observed, which generated POSS crystals. At about 204 min, an L−L phase separation began to take place, generating small droplets dispersed in the epoxy matrix. At advanced conversions, the material exhibited a dual morphology of dispersed POSS crystalline platelets and dispersed droplets. This morphology could be quenched when the reaction at 115 °C was carried out to conversions close to gelation (about 60% conversion), using the conversion vs time curve obtained by FT-NIR provided as Supporting Information.

Figure 8 shows morphologies generated in samples containing different POSS amounts. The presence of POSS crystalline platelets is clearly observed together with a dispersion of (small)

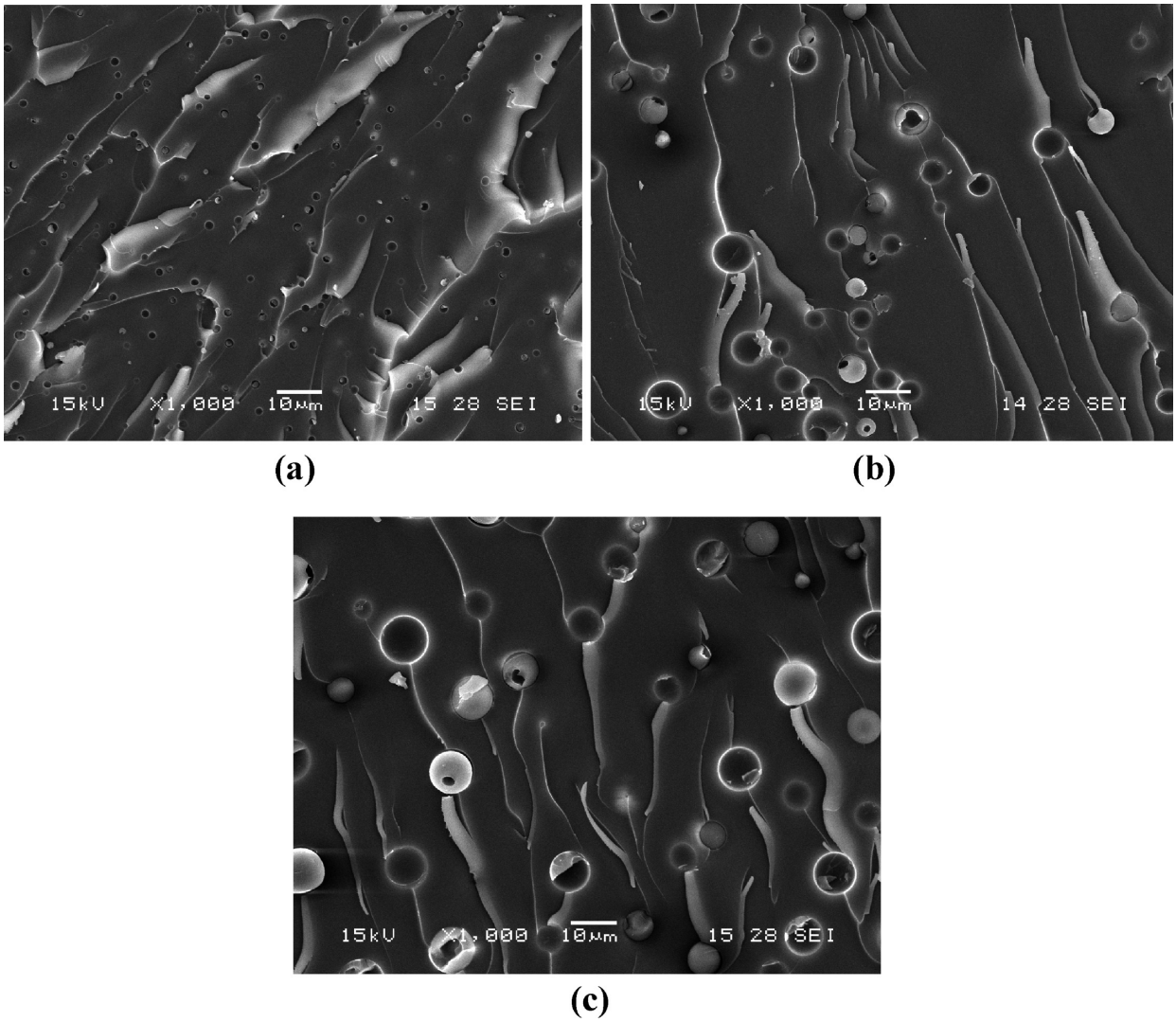

Figure 5. SEM micrographs showing the morphologies generated by an L−L phase separation in POSS−DGEBA/MDEA blends cured at 135 °C and postcured at 190 °C: (a) 5 wt % POSS, (b) 10 wt % POSS, and (c) 15 wt % POSS.

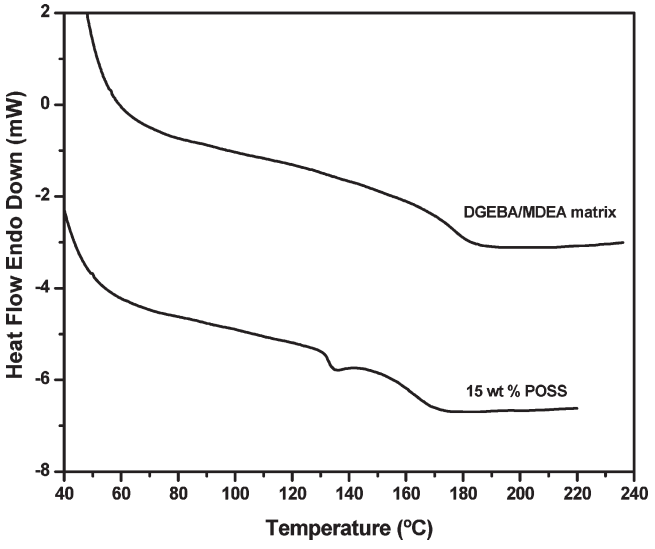

Figure 6. DSC thermograms of the cured DGEBA/MDEA matrix and the blend containing 15 wt % POSS cured at 135 °C and postcured at 190 °C.

spherical POSS-rich domains. This proves that is possible to obtain morphologies that are somewhat similar (except for the nanoscopic size of thickness) to those observed in clay-modified polymers using a bottom-up approach, with POSS replacing the clay. Postcuring at 190 °C and cooling to room temperature did not produce any significant change in morphologies. Figure 8d shows the presence of POSS crystals in a sample containing 5 wt % POSS that was postcured at 190 °C and cooled to room temperature.

In order to build up a thermodynamic model of the process, phase separation times were transformed into phase separation conversions using the conversion vs time curve obtained for the neat matrix at 115 °C. The effect of small POSS amounts on the reaction kinetics was neglected. Table 1 shows the conversions for C−L and L−L phase separations. Although both phase separation processes are well separated in a time scale, they are very close in a conversion scale. The blend containing 10 wt % POSS was already in a metastable region. A very small advance in conversion produced the generation of POSS crystals (the mixing of MDEA with POSS−DGEBA binary solutions was performed in very short times so that the advance in the reaction in this step could be neglected). For the remaining blends, the C−L phase separation was observed at increasing conversions when decreasing the POSS amount.

Thermodynamic Model of the Phase Separation Process. The blend was considered as a pseudobinary system where one component is monodisperse and the other component,

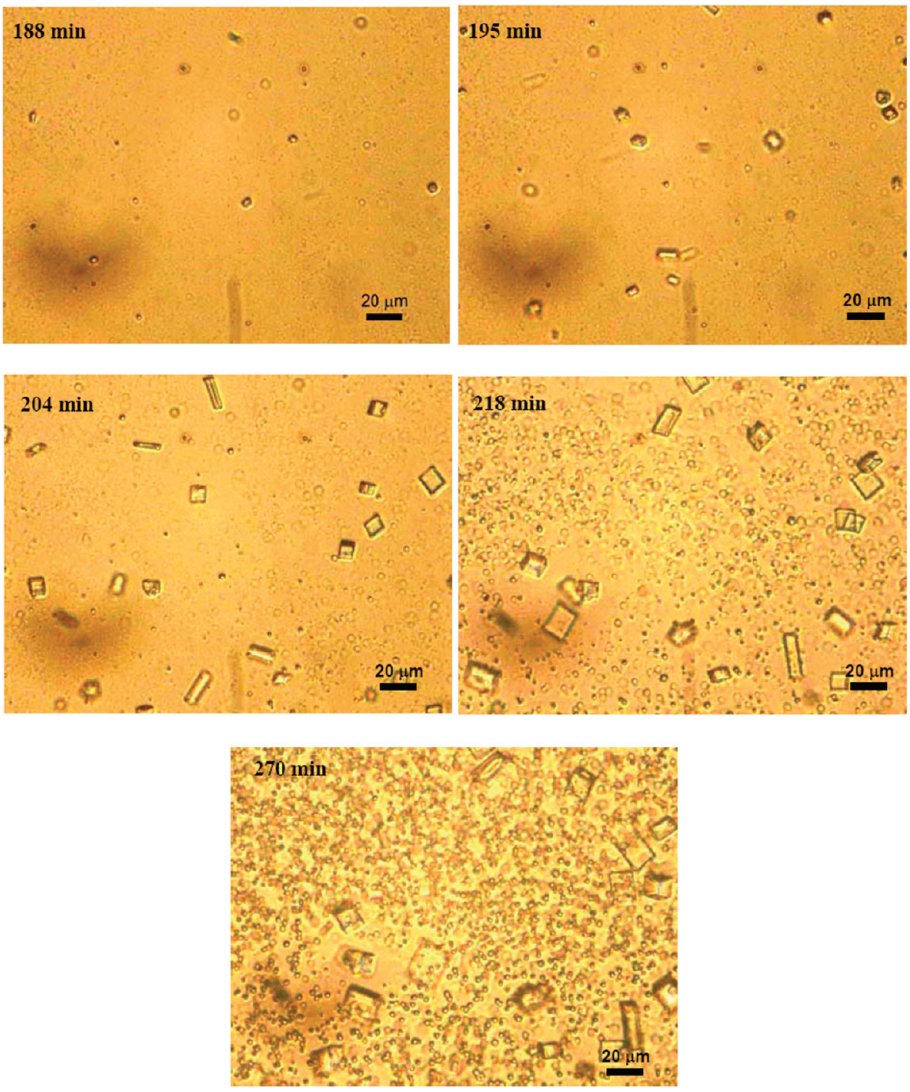

Figure 7. Sequence of the evolution of morphologies observed by TOM in a POSS−DGEBA/MDEA blend with 5 wt % POSS cured at 115 °C.

the pseudocomponent, is polydisperse (distribution of epoxy/amine species varying with conversion). The molar-mass distribution of the DGEBA/MDEA polymer in the pregel stage was calculated from the Stockmayer equation applied to a stoichiometric $A_2 + B_4$ polymerization.[14] This enabled to obtain the number of moles of epoxy−amine species containing m MDEA units and n DGEBA units, $E_{m,n}$, and the volume fraction contributed by these species (neglecting the volume contraction during polymerization), as a function of conversion:

$$\phi_{m,n} = E_{m,n}(mV_{\mathrm{MDEA}} + nV_{\mathrm{DGEBA}})\phi_{\mathrm{E-A}}/[(\mathrm{MDEA})_0 V_{\mathrm{MDEA}} + (\mathrm{DGEBA})_0 V_{\mathrm{DGEBA}}] \quad (1)$$

where $\phi_{\mathrm{E-A}} = \sum_m \sum_n \phi_{m,n} = 1 - \phi_{\mathrm{POSS}}$ is the volume fraction of the epoxy/amine component in the blend, and $V_{\mathrm{MDEA}} = 304.4\ \mathrm{cm^3/mol}$ and $V_{\mathrm{DGEBA}} = 297.9\ \mathrm{cm^3/mol}$ are the molar volumes of both monomers.

The thermodynamic analysis for the L−L phase separation was performed using the Flory−Huggins (F−H) equation:

$$(V_r/RT)\Delta G = \sum_m \sum_n (\phi_{m,n}/r_{m,n}) \ln \phi_{m,n} + (\phi_{\mathrm{POSS}}/r_{\mathrm{POSS}}) \ln \phi_{\mathrm{POSS}} + g(T, \phi_{\mathrm{POSS}})\phi_{\mathrm{E-A}}\phi_{\mathrm{POSS}} \quad (2)$$

where ΔG is the free energy per unit volume, R is the gas constant, T is temperature, V_r is the reference volume taken as the one of MDEA, $r_{m,n} = (mV_{\mathrm{MDEA}} + nV_{\mathrm{DGEBA}})/V_r$ is the ratio of the molar volume of the generic $E_{m,n}$ species with respect to the reference volume, and r_{POSS} represents the ratio of the molar volume of POSS ($V_{\mathrm{POSS}} = 817.2\ \mathrm{cm^3/mol}$) with respect to the reference volume. The following functionality of the interaction parameter, defined by Prausnitz and co-workers,[15] already employed to model phase separation induced by polymerization,[16,17] was used:

$$g(T, \phi_{\mathrm{POSS}}) = (a + b/T)[1/c(1 - \phi_{\mathrm{POSS}})] \ln[(1 - c\phi_{\mathrm{POSS}})/(1 - c)] \quad (3)$$

where a, b, and c are adjustable parameters. This interaction parameter is related to the chi parameter defined in the expression of chemical potentials by[15,18]

$$\chi(T, \phi_{\mathrm{POSS}}) = g(T, \phi_{\mathrm{POSS}}) - \phi_1 g'(T, \phi_{\mathrm{POSS}}) = (a + b/T)/(1 - c\phi_{\mathrm{POSS}}) \quad (4)$$

where the prime denotes the first derivative with respect to the volume fraction of POSS.

The analysis of phase separation in the course of polymerization required to solve the F−H equation for a particular

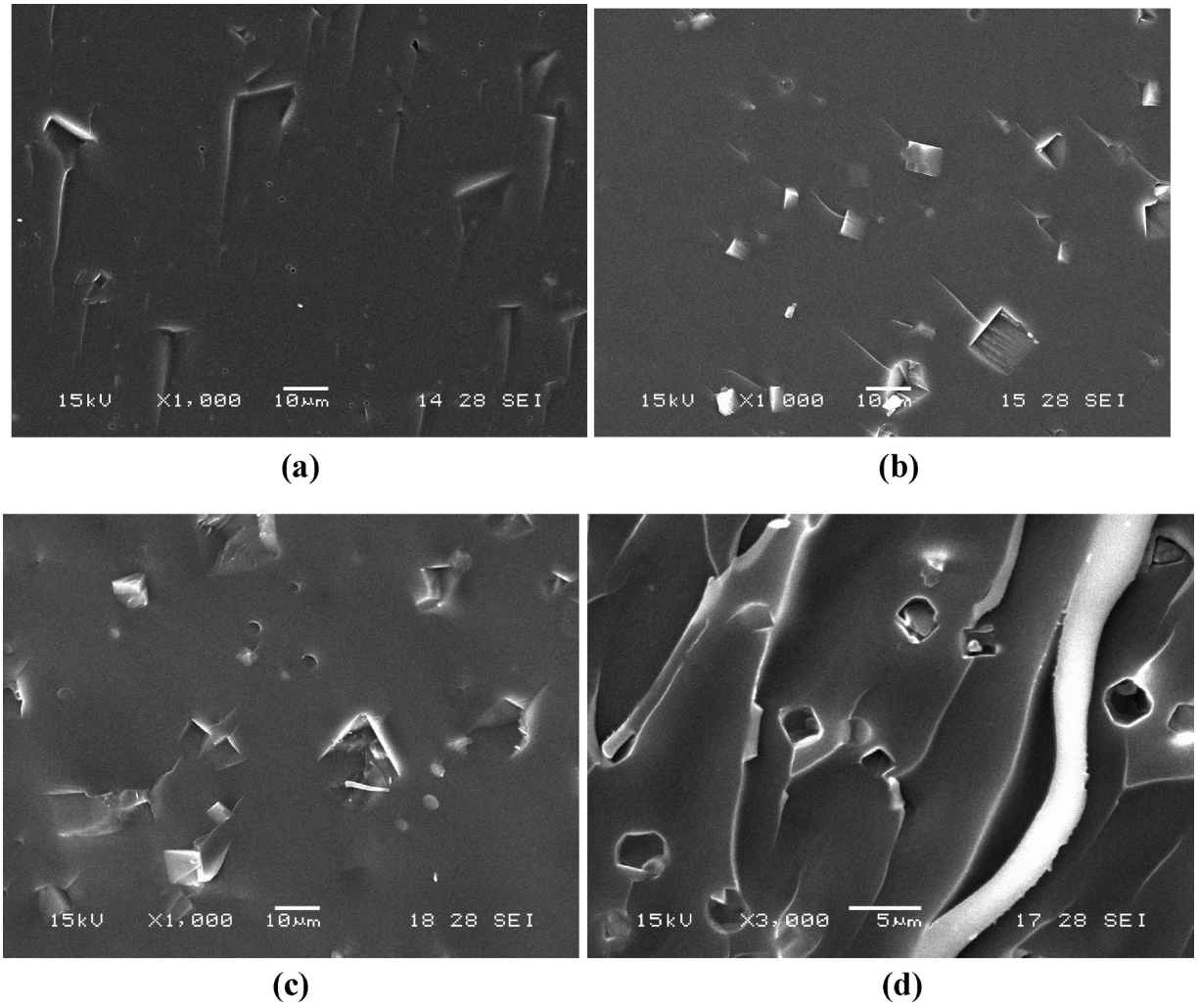

Figure 8. SEM micrographs showing the morphologies generated in POSS−DGEBA/MDEA blends cured at 115 °C: (a) 3.5 wt % POSS, (b) 7.5 wt % POSS, (c) 10 wt %, (d) 5 wt % POSS after postcure at 190 °C.

Table 1. Conversions for the C−L and L−L Phase Separations in a POSS−DGEBA/MDEA Blend Polymerized at 115 °C

wt % POSS	conversion (L−C phase separation)	conversion (L−L phase separation)
3.5	0.16	0.20
5	0.06	0.10
7.5	0.01	0.04
10	< 0.01	0.03

conversion. The distribution of $E_{m,n}$ species was truncated at a value such that the difference of mass-average molar masses of the truncated distribution and the exact distribution was negligible. Cloud-point curves were obtained using standard procedures, including the introduction of two separation factors.[15,19−22] The numerical solution was performed using Mathcad 13 and a Levenberg−Marquardt program to obtain the best set of adjustable parameters

The C−L equilibrium between pure crystalline POSS and the solution was calculated from the classic equations developed by Flory and extended to a polydisperse solvent using the Flory−Huggins model.[23] The melting temperature of pure POSS was taken as 149 °C (maximum melting temperature observed when POSS was crystallized in mass), and the heat of fusion was equal to 15.9 J/g.[1] The same interaction parameter was used to model C−L and L−L equilibria.

A reasonable fitting of the melting curve was obtained using the following parameters in the Prausnitz' equation

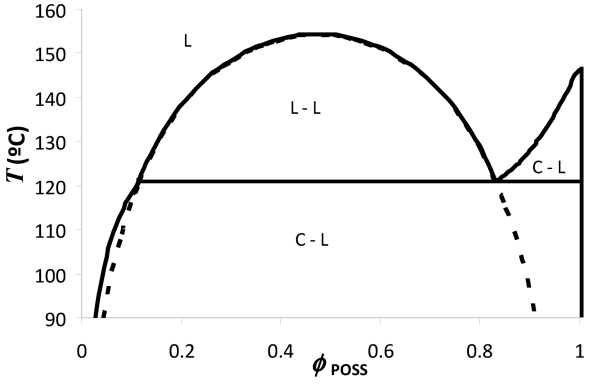

Figure 9. Phase diagram of the POSS−DGEBA/MDEA blend before reaction.

($a = -3.482$, $b = 2415$, and $c = -0.721$). The same parameters were used to predict the L−L equilibrium. Figure 9 shows the phase diagram of the POSS−DGEBA/MDEA blend before reaction. Stable L−L and C−L equilibria are indicated by full lines while metastable L−L equilibrium is shown by a dashed line.

Figure 10 shows the same phase diagram in the region of ϕ_{POSS} comprised between 0 and 0.20. A reasonable prediction of the melting curve was obtained. When the initial system was subcooled below the melting curve, crystallization of

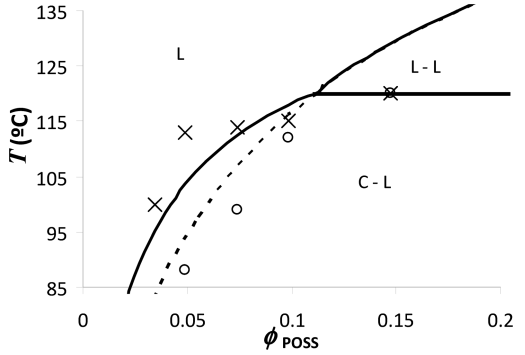

Figure 10. Phase diagram of the POSS−DGEBA/MDEA blend before reaction in the region of ϕ_{POSS} comprised between 0 and 0.20 (crosses represent experimental melting temperatures and circles are experimental values of the L−L phase separation).

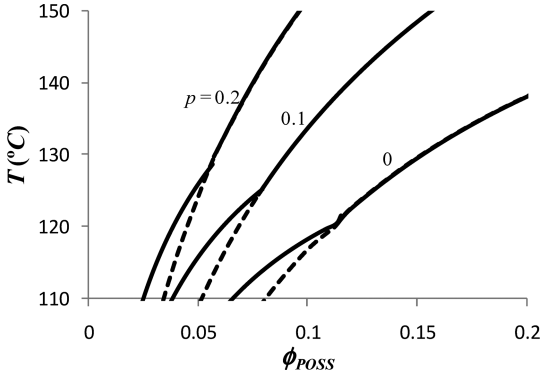

Figure 11. Evolution of the phase diagram as a function of conversion (p).

POSS began to take place, shifting the composition of the continuous phase to lower POSS concentrations. At a particular temperature the L−L metastable region was attained. According to the empirical Ostwald's rule of stages, the metastable phase (liquid droplets) is formed first, followed by the generation of the thermodynamic stable phase (crystallization inside liquid droplets).[24,25]

The experimental points observed for the L−L phase separation are slightly shifted to the right of the theoretical curve. This is expected because pure POSS crystals are separated before the L−L phase separation, shifting the actual composition of the residual liquid to the left. This approaches the experimental points to the theoretical curve. As shown in Figure 9, the generated droplets have a composition very rich in POSS (right branch of the theoretical L−L curve). At these composition POSS crystallization should rapidly take place inside the droplets. Therefore, the material exhibits a dispersion of POSS crystalline platelets and of spherical droplets containing POSS crystals. The existence of two phase separation processes, C−L and L−L, occurring in series is supported by the calculated phase diagrams shown in Figures 9 and 10.

We will now analyze the phase separation in the course of polymerization. Figure 11 shows the predicted evolution of the phase diagram as a function of conversion (p). As conversion increases, experimental points that were initially located in the homogeneous region enter the immiscibility region of the phase diagram. Those located at 115 °C are first reached by the C−L curve and then by the metastable L−L curve. This provides a qualitative explanation of C−L and L−L phase separation occurring in series at this temperature. At 135 °C, experimental points initially located in the homogeneous region enter the L−L phase separation region

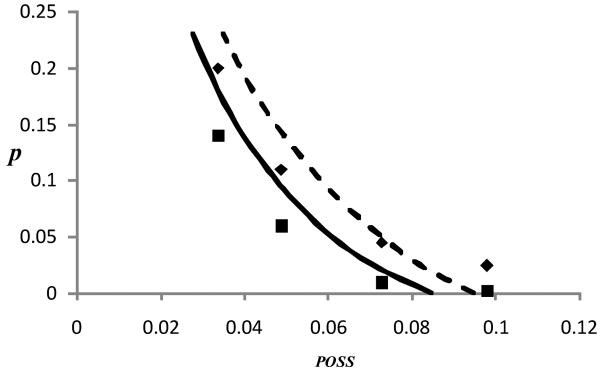

Figure 12. Fitting of predicted C−L and L−L phase separation conversions at 115 °C with experimental points (full line is the predicted C−L curve, and corresponding experimental points are indicated by squares; dashed line is the predicted L−L curve, and corresponding experimental points are indicated by diamonds).

at particular conversions. This provides a qualitative explanation of the fact that only an L−L phase separation process was observed at this temperature. Crystallization took place inside the droplets when cooling to room temperature, as predicted by the phase diagram.

A reasonable fitting of predicted C−L and L−L phase separation conversions at 115 °C with experimental points is shown in Figure 12.

Conclusions

We showed the possibility of generating a dispersion of POSS crystalline platelets in a thermosetting polymer using a polymerization-induced phase separation in the C−L region of the phase diagram. For the selected epoxy−amine formulation, an L−L phase separation occurred subsequently to the C−L phase separation, generating a dispersion of spherical POSS-rich domains. This secondary phase separation could have been avoided by a better matching of chemical structures of the organic groups present in the POSS structure and those of the selected monomers so as to bury the L−L immiscibility region inside the C−L region.

Generated morphologies can be compared to those observed in dispersions of intercalated clays in polymers (micrometer-size platelets dispersed in a polymeric matrix). However, the nanosize thickness of completely exfoliated clays could not be produced when crystallizing POSS in a polymer matrix. This remains as an open question for further research in the field. A possible approach relies on the use of inorganic nanoparticles that can self-assemble as crystalline platelets with a nanosize thickness during polymerization.

Acknowledgment. C. Di Luca thanks the Comisión de Investigaciones Científicas de la Provincia de Buenos Aires for a scholarship for advanced undergraduate students. The financial support of the following Argentine institutions is gratefully acknowledged: National Research Council (CONICET), University of Mar del Plata, and National Agency for the Promotion of Science and Technology (ANPCyT).

Supporting Information Available: Conversion vs time curves for the neat matrix at 115 and 135 °C, determined by FT-NIR. This material is available free of charge via the Internet at http://pubs.acs.org.

References and Notes

(1) Abad, M. J.; Barral, L.; Fasce, D. P.; Williams, R. J. J. *Macromolecules* **2003**, *36*, 3128.
(2) Ni, Y.; Zheng, S.; Nie, K. *Polymer* **2004**, *45*, 5557.

(3) Liu, H.; Zheng, S.; Nie, K. *Macromolecules* **2005**, *38*, 5088.
(4) Liu, Y. L.; Chang, G. P. *J. Polym. Sci., Part A: Polym. Chem.* **2006**, *44*, 1869.
(5) Zucchi, I. A.; Galante, M. J.; Williams, R. J. J.; Franchini, E.; Galy, J.; Gérard, J. F. *Macromolecules* **2007**, *40*, 1274.
(6) Oyanguren, P. A.; Frontini, P. M.; Williams, R. J. J.; Girard-Reydet, E.; Pascault, J. P. *Polymer* **1996**, *37*, 3079.
(7) Oyanguren, P. A.; Frontini, P. M.; Williams, R. J. J.; Vigier, G.; Pascault, J. P. *Polymer* **1996**, *37*, 3087.
(8) Goosens, S.; Goderis, B.; Groeninckx, G. *Macromolecules* **2006**, *39*, 2953.
(9) Goosens, S.; Groeninckx, G. *Macromolecules* **2006**, *39*, 8049.
(10) Goosens, S.; Groeninckx, G. *J. Polym. Sci., Part B: Polym. Phys.* **2007**, *45*, 2456.
(11) Salmon, N.; Carlier, V.; Schut, J.; Remiro, P. M.; Mondragon, I. *Polym. Int.* **2005**, *54*, 667.
(12) Zucchi, I. A.; Hoppe, C. E.; Galante, M. J.; Williams, R. J. J.; López-Quintela, M. A.; Matějka, L.; Slouf, M.; Pleštil, J. *Macromolecules* **2008**, *41*, 4895.
(13) Williams, R. J. J.; Rozenberg, B. A.; Pascault, J. P. *Adv. Polym. Sci.* **1997**, *128*, 95.
(14) Peebles, L. H. *Molecular Weight Distribution in Polymers*; Wiley-Interscience: New York, 1971.
(15) Bae, Y. C.; Shim, J. J.; Soane, D. S.; Prausnitz, J. M. *J. Appl. Polym. Sci.* **1993**, *47*, 1193.
(16) Zucchi, I. A.; Galante, M. J.; Borrajo, J.; Williams, R. J. J. *Macromol. Chem. Phys.* **2004**, *205*, 676.
(17) Soulé, E. R.; Eliçabe, G. E.; Borrajo, J.; Williams, R. J. J. *Ind. Eng. Chem. Res.* **2007**, *46*, 7535.
(18) Mumby, S. J.; Sher, P. *Macromolecules* **1994**, *27*, 689.
(19) Riccardi, C. C.; Borrajo, J.; Williams, R. J. J. *Polymer* **1994**, *35*, 5541.
(20) Shirataki, H.; Matsuda, S.; Kamide, K. *Br. Polym. J.* **1990**, *23*, 285.
(21) Shirataki, H.; Matsuda, S.; Kamide, K. *Br. Polym. J.* **1990**, *23*, 299.
(22) Kamide, K.; Matsuda, S.; Shirataki, H. *Eur. Polym. J.* **1990**, *26*, 379.
(23) Champetier, G.; Monnerie, L. *Introducción a la Química Macromolecular*; Espasa-Calpe: Madrid, 1973.
(24) Putnis, A. *Introduction to Mineral Sciences*; Cambridge University Press: Cambridge, 1992.
(25) Cheng, S. Z. D. *Phase Transitions in Polymers*; Elsevier: Amsterdam, 2008.